

DETECTION OF X-RAYS FROM THE SYMBIOTIC STAR V1329 CYG

MATTHIAS STUTE^{1,2}, GERARDO J. M. LUNA³, AND JENNIFER L. SOKOLOSKI⁴

Received 2010 September 27; accepted 2011 February 3

ABSTRACT

We report the detection of X-ray emission from the symbiotic star V1329 Cyg with XMM-Newton. The spectrum from the EPIC pn, MOS1 and MOS2 instruments consists of a two-temperature plasma with $kT_1 = 0.11^{+0.02}_{-0.02}$ keV and $kT_2 = 0.93^{+0.12}_{-0.14}$ keV. Unlike the vast majority of symbiotic stars detected in X-rays, the soft component of the spectrum seems to be absorbed only by interstellar material. The shock velocities corresponding to the observed temperatures are about 300 km s^{-1} and about 900 km s^{-1} . We did not find either periodic or aperiodic X-ray variability, with upper limits on the amplitudes of such variations being 46% and 16% (rms), respectively. We also did not find any ultraviolet variability with an rms amplitude of more than approximately 1%. The derived velocities and the unabsorbed nature of the soft component of the X-ray spectrum suggest that some portion of the high energy emission could originate in shocks within a jet and beyond the symbiotic nebula. The lower velocity is consistent with the expansion velocity of the extended structure present in HST observations. The higher velocity could be associated with an internal shock at the base of the jet or with shocks in the accretion region.

Subject headings: binaries: symbiotic – stars: individual (V1329 Cyg=HBV 475) – stars: white dwarfs – X-rays: stars – ISM: jets and outflows

1. INTRODUCTION

V1329 Cygni (=HBV 475) is one of a small number of symbiotic novae (Mürset & Nussbaumer 1994) that have outbursts of 3 to 7 mag and return to their previous brightness only slowly over decades. The canonical model (e.g. Baratta & Viotti 1990) for symbiotic novae involves a hot white dwarf star that has a surface thermonuclear flash, with the fuel supplied by a red giant companion. The only recorded major outburst of V1329 Cyg began in about 1965 and reached B magnitude < 11.5 mag in October 1966. Some time elapsed between discovery as an eruptive object (Kohoutek 1969; Kohoutek & Bossen 1970) and recognition that it is a binary, with the object first being called a proto-planetary nebula (Crampton et al. 1970). The photographic brightness dropped to $m_V < 16$ mag over the past century, with several abrupt drops of as much as another 2.5 mag between 1925 and 1962. These repeated with a period of 950–959 days and were explained as the eclipses of the hot component by the red giant (Stienon et al. 1974; Grygar et al. 1979). Schild & Schmid (1997) improved the determination of the orbital period to 956.5 days and found from polarimetry an inclination of 86 ± 2 degrees. From optical and UV emission lines, orbital parameters of the hot component have been determined yielding minimum masses of about 0.71 and $2 M_\odot$ for the white dwarf and red giant, respec-

tively (Schild & Schmid 1997). These authors derived an E_{B-V} value of 0.6, corresponding to $n_H = 2.3 \times 10^{21} \text{ cm}^{-2}$ (using the conversion factor of Groenewegen & Lamers 1989).

About 200 symbiotic stars are known (e.g. Belczynski et al. 2000), but jets have been detected at different wavelengths only in 10 of them (Brocksopp et al. 2004). V1329 Cygni is a member of this list, since Brocksopp et al. (2003) found two peaks and extended emission in HST WFPC2 snapshot images taken in October 1999 with F502N and F656N filters. These were separated by about 950 AU, assuming a distance of 3.4 kpc as given by Mürset & Nussbaumer (1994). After comparison with HST images of Schild & Schmid (1997) taken in July 1991, they derived an expansion velocity of $260 \pm 50 \text{ km s}^{-1}$, suggesting that this mass ejection was not associated with the nova outburst in 1965, but with an event in 1982. As an additional riddle, the position angle of the orbital plane of $11 \pm 2^\circ$ determined by Schild & Schmid (1997) furthermore suggests that the mass ejection occurred *along* the orbital plane, instead of perpendicular to it as expected for a jet. Using the ephemeris of Schild & Schmid (1997)

$$\text{JD}_{\min} = 2444890.0 + 956.5 \times E, \quad (1)$$

the system was at phase 0.733 during the observations of Schild & Schmid (1997) and at phase 0.880 during that of Brocksopp et al. (2003). Whether the different appearance of the extended [OIII] emission is due to this slightly different orbital phase and thus a changed ionisation structure in the stellar environment, or due to real expansion of the gas inside a wind or jet, is unknown. We also have to note that Schild & Schmid (1997) used the FOC camera with filter F501N, while Brocksopp et al. (2003) used the WFPC2 camera with filter F502N, thus different filters with different properties.

matthias.stute@tat.physik.uni-tuebingen.de

¹ Institute for Astronomy and Astrophysics, Section Computational Physics, Eberhard Karls Universität Tübingen, Auf der Morgenstelle 10, 72076 Tübingen, Germany

² Dipartimento di Fisica Generale "A. Avogadro", Università degli Studi di Torino, Via Pietro Giuria 1, 10125 Torino, Italy

³ Harvard-Smithsonian Center for Astrophysics, 60 Garden St. MS 15, Cambridge, MA, 02138, USA

⁴ Columbia Astrophysics Laboratory, 550 W. 220th Street, 1027 Pupin Hall, Columbia University, New York, NY 10027, USA

Table 1
Observations on May 02/03, 2009 (ObsID: 0604920301)

Instrument	Filter	Duration	UT Start	UT Stop
pn	Medium	57434	11:00:56	02:58:10
MOS1	Medium	59021	10:38:33	03:02:14
MOS2	Medium	59027	10:38:33	03:02:20
OM	U	10× ~1500	10:47:01	16:15:16
	UVW1	10× ~1500	16:50:37	21:48:52
	UVM2	10× ~1500	21:54:13	03:04:49

X-ray observations provide a direct probe of the two most important components of jet-driving systems: the bow and internal shocks of the jet emitting soft X-rays and the central parts of the jet engine, where gas is being accreted to power the jet, leading to hard and/or super-soft X-ray emission. Currently R Aqr (Kellogg et al. 2001, 2007) and CH Cyg (Galloway & Sokoloski 2004; Karovska et al. 2007, 2010) are the only two jets from symbiotic stars that have been resolved in X-rays. All objects with jets, detected in other wavelength, when observed in X-rays, show soft components with $kT < 2$ keV (additionally to sometimes present *super-soft* emission): R Aqr (Kellogg et al. 2001, 2007), CH Cyg (Galloway & Sokoloski 2004; Karovska et al. 2007, 2010), MWC 560 (Stute & Sahai 2009), RS Oph (Luna et al. 2009), AG Dra (Gonzalez-Riestra et al. 2008), Z And (Sokoloski et al. 2006). The three objects CH Cyg, R Aqr, MWC 560 also emit hard components (Mukai et al. 2007; Nichols et al. 2007; Stute & Sahai 2009). Z And showed hard emission in one of three observations only (Sokoloski et al. 2006).

The paper is organized as follows: in Section 2, we show details of the observations and the analysis of the data. After that we describe the results in Section 3. We end with a discussion and conclusions in Sections 4 and 5.

2. OBSERVATION AND ANALYSIS

We observed the field of V1329 Cyg with *XMM-Newton* in 2009 (Table 1) using the EPIC instrument operating in full window mode and with the medium thickness filter. Simultaneously, we used the Optical Monitor OM. All the data reduction was performed using the Science Analysis Software (SAS) software package⁵ version 8.0. We removed event at periods with high background levels from the pipeline products selecting events with pattern 0–4 (only single and double events) for the pn and pattern 0–12 for the MOS, respectively, and applying the filter FLAG=0. The resulting exposure time after these steps is 37.6 ks.

The source spectra and light curves were accumulated from a circular region of 12" radius (240 pixels, Fig. 1) centered on V1329 Cyg using the coordinates from SIMBAD. The background spectra and light curves were extracted from a source-free region on the same chips taken within an circle of 30" radius (600 pixels). Spectral redistribution matrices and ancillary response files were generated using the SAS scripts `rmfgen` and `arfgen`, and spectra grouped with a minimum of 25 counts per energy bin were fed into the spectral fitting package XSPEC⁶

⁵ <http://xmm.vilspa.esa.es/>

⁶ <http://heasarc.gsfc.nasa.gov/docs/xanadu/xspec/>

v12.5.1. For timing analysis, photon arrival times were converted to the solar system barycenter using the SAS task `barycen`.

3. RESULTS

3.1. Images

We detected V1329 Cyg with each of the instruments aboard XMM-Newton. The total numbers of counts in the EPIC pn, MOS1, and MOS2 cameras were 329, 84, and 107, respectively (Fig. 1). For comparison, the total numbers counts expected due to background radiation alone were 83, 36, and 20 for the three X-ray instruments. The average magnitudes in the optical filters U, UVW1 and UVM2 are 12.32, 12.34 and 13.35, respectively. The X-ray images of V1329 Cyg show a point source morphology. In order to assess the possibility of extended emission, we constructed radial profiles from the images using the SAS task `eradial` (a routine to extract a radial profile of a source in an image field and to fit a point spread function [PSF] to it) keeping the centroid fixed at the source position of V1329 Cyg and choosing a step size of two pixels. With this method, we did not find any evidence for extended X-ray emission.

3.2. Spectra

The spectrum of V1329 Cyg is relatively soft with photons having energies of < 2 keV (Fig. 2). It is well described ($\chi^2 = 1.10$, 6 d.o.f.) by a two-temperature plasma model with N overabundant by a factor of ≈ 4 in the softer component compared to solar values (Anders & Grevesse 1989) in order to explain the high flux around 0.4 keV (`vapex` in XSPEC). For the soft component, the fit is consistent with no *internal* absorption, with N_H in the range $(0 - 5) \times 10^{21} \text{ cm}^{-2}$. For the hard component, we find $N_H = 9_{-0.32}^{+4.3} \times 10^{21} \text{ cm}^{-2}$. These values include internal absorption as well as interstellar absorption which in the direction of the source is about $2.3 \times 10^{21} \text{ cm}^{-2}$. The fit is slightly worse ($\chi^2 = 1.27$, 4 d.o.f.) including (non-vanishing) absorption. The temperature of the cooler component is $kT_1 = 0.11_{-0.02}^{+0.02}$ keV, while the temperature of the hotter component is $kT_2 = 0.93_{-0.14}^{+0.12}$ keV. The flux of the hotter component is three times lower than that of the soft component. The total model flux between 0.3 and 2 keV is $1.21 \times 10^{-14} \text{ erg s}^{-1} \text{ cm}^{-2}$. With the assumed distance of 3.4 kpc, this flux corresponds to a luminosity of $1.7 \times 10^{31} \text{ erg s}^{-1}$.

The slope of the ultraviolet spectral energy distribution indicates that the optical flux is dominated by nebular emission and the red giant (Fig. 3). The flux level of blackbody emission corresponding to a white dwarf with a radius of $8 \times 10^8 \text{ cm}$ at a distance of 3.4 kpc with an effective temperature of 145000 K (Mürset et al. 1991) is lower than the measured fluxes by 1–2 orders of magnitude.

3.3. Light curves

We examined time series binned at 3000s in the energy range 0.3–2 keV (Fig. 4) and the OM photometry with exposure times of about 1500s (Fig. 5). We chose the bin size for the X-ray light curve to produce at least roughly 25 counts per bin while still providing time resolution

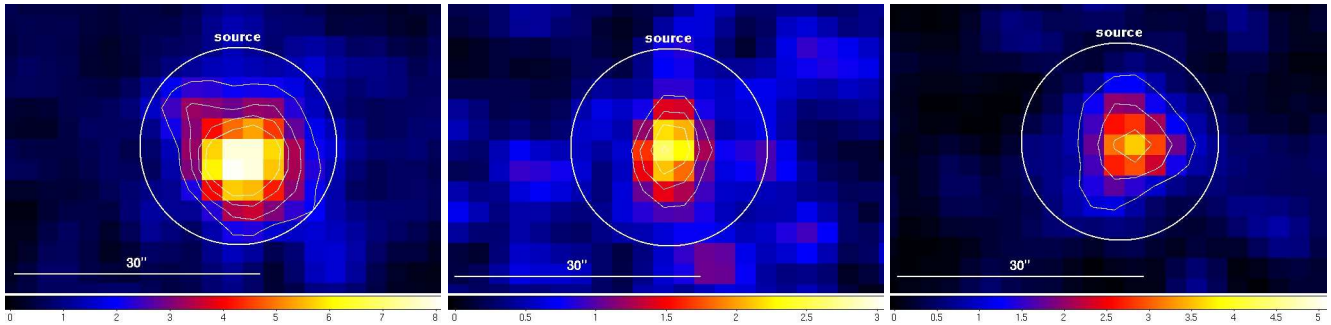


Figure 1. Left: *XMM-Newton* EPIC pn image (detail) of the region around V1329 Cyg in the 0.3–2 keV range. Also shown is the extraction region for the source events. Contour levels are 2, 3, 4 and 5 counts per pixel; middle: *XMM-Newton* EPIC MOS1 image of the same region. Contour levels are 1.5, 2 and 2.5 counts per pixel; right: *XMM-Newton* EPIC MOS2 image of the same region. Contours are 1, 2, 3 and 4 counts per pixel.

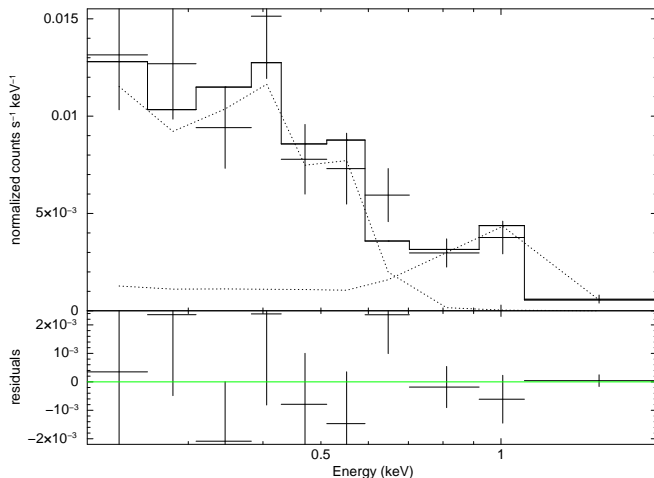


Figure 2. Observed spectrum of V1329 Cyg together with a model consisting of two absorbed thermal components (*vaptec*; dotted lines) with variable abundances.

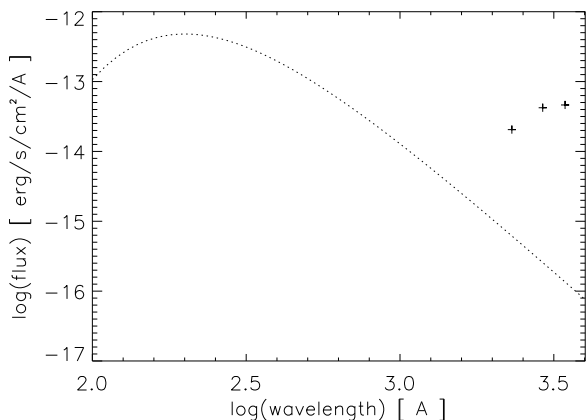


Figure 3. Spectral energy distribution in the optical filters U, UVW1 and UVM2. Also plotted is blackbody emission representing a white dwarf with a temperature of 145000 K and radius of 8×10^8 cm. The slope and flux level of the spectral energy distribution indicate that the optical flux is dominated by nebular emission and the red giant.

of less than an hour. The X-ray and two of the optical light curves are consistent with a constant flux. The measured rms variations, those expected from Poisson statistics, and the ratios of these two quantities are listed in Table 2. s and s_{exp} are given in percentage of the

mean value. Only in filter UVW1, the ratio $s/s_{exp} > 1$ indicates variability.

We also searched for modulated emission in the light curves. Using the arrival times of the source events, we calculated the Z_1^2 (Rayleigh) statistic (Buccheri et al. 1983) in the frequency range $f_{min} = 1/T_{exp}$ to $f_{max} = 1/2 t_{frame}$ with $\Delta f = 1/T_{exp}$; where T_{exp} is the effective exposure time of 37.6 ks and t_{frame} is the readout time (73 ms in the case of XMM). The value of Z_1^2 needed to detect pulsation with a probability P is given by

$$Z_1^2 > 2 \times \ln\left(\frac{T_{exp} \times \Delta f}{P}\right). \quad (2)$$

Thus for a 3- σ ($P = 2.699 \times 10^{-3}$) detection, $Z_1^2 > 36.7$ is required. The highest value of Z_1^2 detected in our observation is 27.5, which corresponds only to 1.26- σ . With $N_S=329$ and $N_B=83$ source and background photons detected with the EPIC pn camera respectively, the pulse fraction corresponding to the highest Z_1^2 value detected is

$$\begin{aligned} p &= p_{obs}(N_S + N_B)N_S^{-1} \\ &\approx [2Z_1^2(N_S + N_B)]^{1/2}N_S^{-1} \pm [2(N_S + N_B)]^{1/2}N_S^{-1} \\ &= 0.46 \pm 0.009 \end{aligned} \quad (3)$$

for a nearly sinusoidal signal, where p_{obs} is the pulsed fraction uncorrected for the background contribution. Therefore, our observation is only sensitive to pulse fractions $p \gtrsim 46$ %.

4. DISCUSSION

The X-ray images of V1329 Cyg show a point source morphology; no hints of extended emission are present. In Figure 6, we show *HST* images from Schild & Schmid (1997) and Brocksopp et al. (2003) where extended emission in [OIII] is evident. These authors concluded that the visible optical emission is an expanding jet, however, resulting in the conundrum that the mass ejection occurred *along* the orbital plane.

The two-temperature X-ray emission can be explained in the light of simulations of jets in symbiotic stars (Stute 2006; Stute & Sahai 2007) where soft X-ray emission arises from internal shocks and the bow shock. The velocity of the shock, v_{shock} , can be derived using the measured temperature of the component and the following relation (assuming strong shock conditions):

$$T_{post\ shock} = \frac{3}{16} \frac{\mu m_P}{k_B} v_{shock}^2$$

Table 2
Measured and expected variations and their ratio

Instrument	measured variation s	expected variation s_{exp}	ratio s/s_{exp}
X-ray	39.62 %	38.56 %	1.03
optical U	0.054 %	0.061 %	0.89
optical UVW1	0.095 %	0.025 %	3.77
optical UVM2	0.063 %	0.067 %	0.94

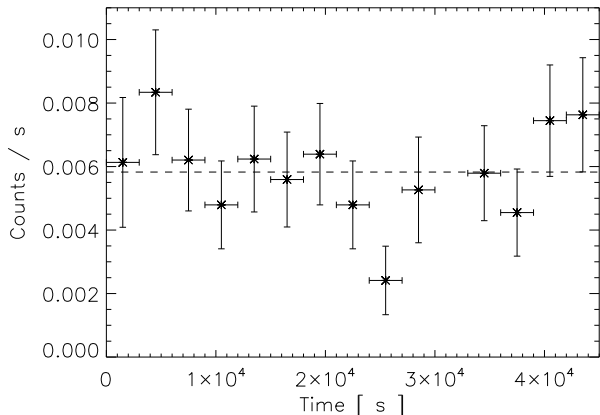


Figure 4. EPIC pn light curve binned at 3000 s in the energy range 0.3–2 keV. The dashed line shows the average count rate. Overall the light curve is consistent with X-ray flux being constant – the ratio of measured rms to that expected from Poisson statistics, s/s_{exp} , is 1.03.

$$= 0.105 \text{ keV} \left(\frac{v_{shock}}{300 \text{ km s}^{-1}} \right)^2 \quad (4)$$

with m_p the proton mass, k_B the Boltzmann constant and $\mu = 0.6$ the mean particle weight. Therefore the soft component temperature corresponds to a shock velocity of about 300 km s^{-1} , consistent with the expansion velocity of $260 \pm 50 \text{ km s}^{-1}$ of the optical extended structure measured by Brocksopp et al. (2003).

Furthermore the temperature of the hot component suggests the presence of another shock with a velocity of about 900 km s^{-1} . The spatial resolution is by far not good enough to further connect the apparent flow in HST observations with our results. However, if the optical extended structure represents a jet, then the second shock could be located at the base of the jet. The harder of the two X-ray components could also arise from the boundary layer between the accretion disk and the white dwarf. Pandel et al. (2005) found that the maximum temperature in a cooling flow representing an optically-thin boundary layer is $kT_{max} = 3/5 kT_{virial}$. The temperature inferred from a single-temperature fit will be lower than kT_{max} . The plasma temperature from single temperature fits to boundary layer emission in Kennea et al. (2009) from RT Cru, T CrB, CH Cyg and SS73 17 are lower than the maximum temperatures determined from cooling flow fits in RT Cru (Luna & Sokolowski 2007), T CrB (Luna et al. 2008) and SS73 17 (Eze et al. 2010). The higher absorbing column in front of the hard component is consistent with this component being closer to the central engine than the lower temperature plasma.

The fact that the soft component of the X-ray spectrum is consistent with no internal absorption can only be explained if the source of the X-ray emission lies out-

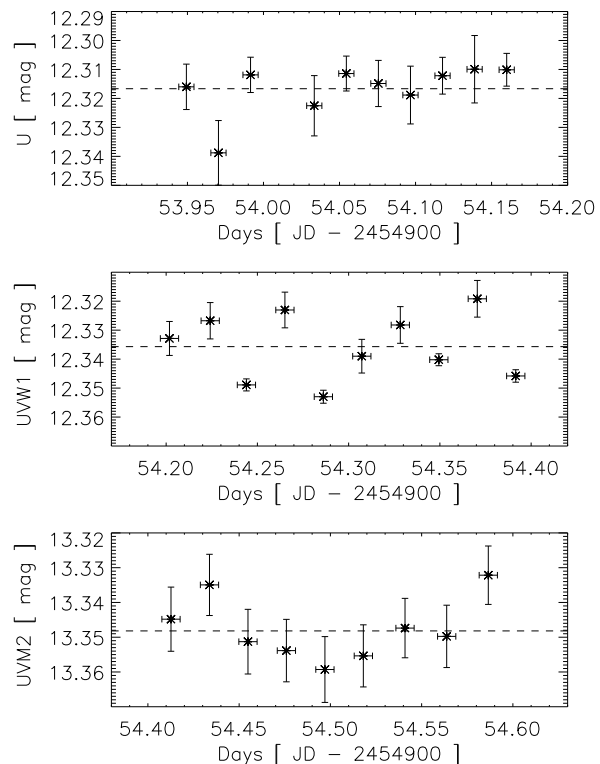


Figure 5. Light curves of the OM exposures for filters U (top, 3440 Å), UVW1 (middle, 2910 Å) and UVM2 (bottom, 2310 Å). The dotted lines show the average magnitude. The light curves for filters U and UVM2 are consistent with a constant flux ($s/s_{exp} = 0.89$ and 0.94), while $s/s_{exp} = 3.77$ for the UVW1 filter indicates variability.

side of the symbiotic nebula with a typical size of a few AU. In contrast, almost all symbiotic stars detected in X-rays show spectra absorbed by column densities of a few 10^{21} to 10^{23} cm^2 (e.g. Luna & Sokolowski 2007; Kennea et al. 2009).

The over-abundance of N by a factor of ≈ 4 has some implications for the origin of the shocked material. Schmid & Schild (1990) find in V1329 Cyg an enhancement factor of about 10 in nitrogen in the symbiotic nebula from optical, NIR and UV spectroscopy. The mean abundances found in M giants show an over-abundance of N by a factor of 3.5 compared to solar values (Smith & Lambert 1985, 1986), due to the conversion of carbon into nitrogen and mixing into the atmosphere of the red giant (Nussbaumer et al. 1988). Larger values may be attributed to more advanced nuclear burning stages. Therefore the shocked material in the softer component was probably initially part of the red giant wind,

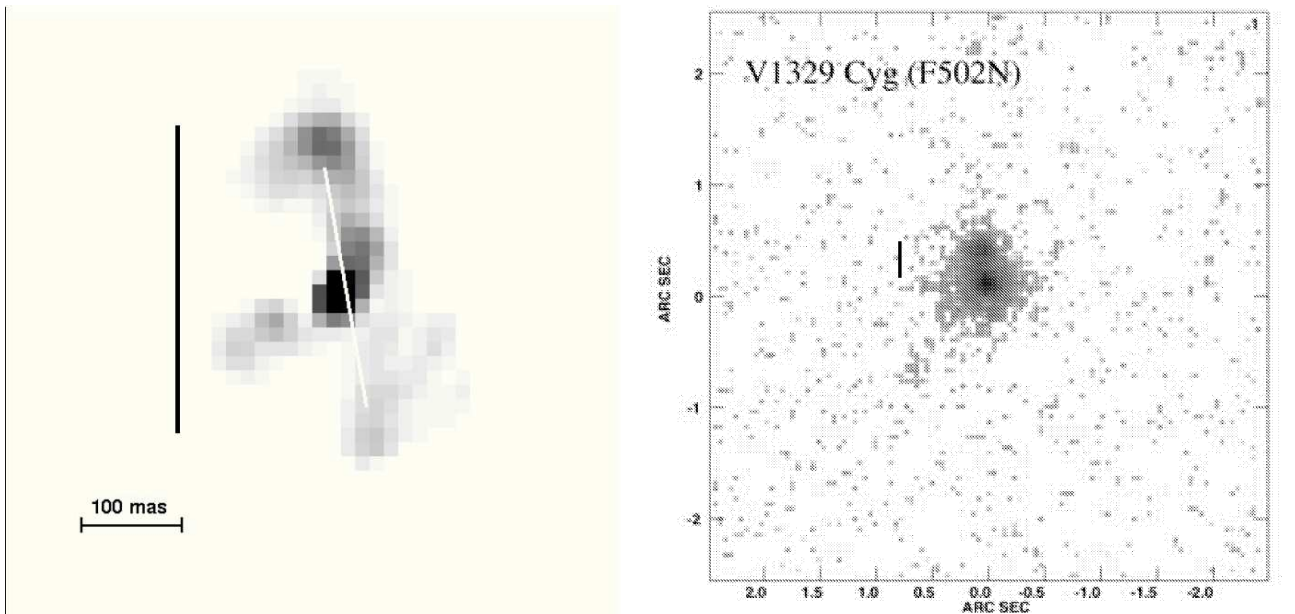


Figure 6. Left: *HST* image in the filter F501N of the region around V1329 Cyg from Schild & Schmid (1997). The orientation of the orbital plane is indicated by the white line; right: *HST* image in the filter F502N of the same region from Brocksopp et al. (2003). For comparison, a scale of 300 mas has been added in both images.

which has not been further reprocessed during thermonuclear burning close to the white dwarf (Schmid & Schild 1990) and has been ejected outside of the symbiotic nebula within a jet.

The possible lack of short term variability in the X-ray light curve may support the above scenario. Variability with time scales of minutes to hours is typically observed in symbiotics where X-ray originate in the accretion flow (e.g. SS73 17, Eze et al. 2010, or CH Cyg, Mukai et al. 2007). However, because the X-ray count rate from V1329 Cyg leads to large error bars, we cannot definitely exclude flickering. Variability is statistically detected only in the UVW1 band at 2910 Å and the rms amplitude of this variability is only 1%.

5. CONCLUSION

We report the detection for the first time of X-ray emission from the symbiotic star V1329 Cyg which was not previously detected by *ROSAT* due to its low X-ray flux. The observed X-ray temperatures and especially the unabsorbed nature of the soft component of the X-ray spectrum indicate that some of the X-ray emission might originate in shocks inside a jet outside the symbiotic nebula. In this regard, V1329 Cyg adds to the small but growing group of jet-driving symbiotics with X-ray emission.

MS wishes to thank Hans Martin Schmid for fruitful discussions. This work is based on observations obtained with *XMM-Newton*, an ESA science mission with instruments and contributions directly funded by ESA Member States and the USA (NASA). We thank NASA for funding this work through XMM-Newton AO-8 awards NNX09AP88G to GJML and JLS, and NNX10AK31G to JLS. We also acknowledge helpful comments and suggestions by an anonymous referee.

REFERENCES

- Anders, E., Grevesse, N. 1989, *GeCoA*, 53, 197
 Baratta, G. B., Viotti, R. 1990, *A & A*, 229, 104
 Belczynski K., Mikolajewska J., Munari U., et al. 2000, *A & AS*, 146, 407
 Brocksopp, C., Bode, M. F., Eyres, S. P. S. 2003, *MNRAS*, 344, 1264
 Brocksopp, C., Sokoloski, J. L., Kaiser, C., et al. 2004, *MNRAS*, 347, 430
 Bucheri, R., Bennett, K., Bignami, G. F., et al. 1983, *A & A*, 128, 245
 Crampton, D., Grygar, J., Kohoutek, L., Viotti, R. 1970, *ApL*, 6, 5
 Galloway, D. K., Sokoloski, J. L. 2004, *ApJ*, 613, L61
 Eze, R. N. C., Luna, G. J. M., Smith, R. K. 2010, *ApJ*, 709, 816
 Gonzalez-Riestra, R., Viotti, R. F., Iijima, T., et al. 2008, *A & A*, 481, 725
 Groenewegen, M. A. T., Lamers, H. J. G. L. M. 1989, *A&ASS* 79, 359
 Grygar, J., Hric, L., Chochol, D., Mammano, A. 1979, *Bulletin of the Astronomical Institute of Czechoslovakia*, vol. 30, p.308
 Karovska, M., Carilli, C. L., Raymond, J. C., Mattei, J. A. 2007, *ApJ*, 661, 1048
 Karovska, M., Gaetz, T. J., Carilli, C. L., Hack, W., Raymond, J. C., Lee, N. P. 2010, *ApJ*, 710, 132
 Kellogg, E., Pedelty, J. A., Lyon, R. G. 2001, *ApJ*, 563, 151
 Kellogg, E., Anderson, C., Korreck, K., et al. 2007, *ApJ*, 664, 1079
 Kennea, J. A., Mukai, K., Sokoloski, J. L., Luna, G. J. M., Tueller, J., Markwardt, C. B., Burrows, D. N. 2009, *ApJ*, 701, 1992
 Kohoutek, L., *Information Bulletin on Variable Stars*, 384, 1.
 Kohoutek, L., Bossen, H. 1970, *ApL* 6, 157
 Luna, G. J. M., Sokoloski, J. L. 2007, *ApJ*, 671, 741
 Luna, G. J. M., Sokoloski, J. L., Mukai, K. 2008, *ASP Conf. Ser.* 401, 342
 Luna, G. J. M., Montez, R., Sokoloski, J. L., Mukai, K., Kastner, J. H. 2009, *ApJ*, 707, 1168
 Mukai, K., Ishida, M., Kilbourne, C., et al. 2006, *PASJ*, 59, 177
 Mürset, U., Nussbaumer, H. 1994, *A & A*, 282, 586
 Mürset, U., Nussbaumer, H., Schmid, H. M., Vogel, M. 1991, *A & A* 248, 458
 Nichols, J. S., DePasquale, J., Kellogg, E., et al. 2007, *ApJ*, 660, 651
 Nussbaumer, H., Schild, H., Schmid, H. M., Vogel, M. 1988, *A & A*, 198, 179
 Pandel, D., Cordova, F. A., Mason, K. O., Priedhorsky, W. C., 2005., *ApJ*, 626, 396

- Schild, H., Schmid, H. M. 1997, *A & A*, 324, 606
Schmid, H. M., Kaufer, A., Camenzind, M., et al. 2001, *A & A*, 377, 206
Schmid, H. M., Schild, H. 1990, *MNRAS*, 246, 84
Smith, V. V., Lambert, D. L. 1985, *ApJ*, 294, 326
Smith, V. V., Lambert, D. L. 1986, *ApJ*, 311, 843
Sokoloski, J. L., Kenyon, S. J., Espey, B. R., et al. 2006, *ApJ*, 636, 1002
Stienon, F. M., Chartrand, M. R., III, Shao, C. Y. 1974, *AJ*, 79, 47
Stute, M., 2006, *A & A*, 450, 645
Stute, M., Sahai, R. 2007, *ApJ*, 665, 698
Stute, M., Sahai, R. 2009, *A & A*, 498, 209